ORIGINAL PAPER

Peter Momme · Christian Tegner · C. Kent Brooks
Reid R. Keays

Two melting regimes during Paleogene flood basalt generation in East Greenland: combined REE and PGE modelling

Abstract Previously published platinum group element (PGE) and rare earth element data (REE) from a sample suite of the Palaeogene flood basalts of the East Greenland rifted margin are used to approximate primary magma compositions by numerical models of mantle melting. Both high-Ti and low-Ti basalts are found intercalated in the coastal section "the Sortebre Profile" in central East Greenland, and the apparent lack of mixing between the two series indicates coexistence of two geographically separated melting regions and plumbing systems during continental breakup above the Palaeogene Iceland plume. The lavas show little or no sign of crustal contamination and the limited variation in La/Sm and Cu/Pd ratios can be interpreted to reflect mantle source composition and melting processes. Numerical modelling indicate that the low-Ti series formed by $F \sim 20\%$ melting in a columnar melting regime from a slightly depleted upper mantle source with a relatively normal S-content (~ 180 ppm S). In contrast, the high-Ti series formed by much lower degrees of melting ($F \sim 6\%$) in a spreading-related, triangular melting regime from a relatively S-poor (~ 100 ppm S) source. The low-Ti suite was S-undersaturated at the stage of melt segregation from a shallow mantle source due to the high degree of melting. In contrast, the high-Ti suite probably formed from a S-poor source where some low degree melt batches were S-saturated at the stage of deep segregation in distal parts of the triangular melting regime. This suite shows a geochemical high pressure garnet-signature and adiabatic decompression could therefore have played a role in keeping the mantle-derived S in solution before Fe-enrichment related to fractional crystallisation also increased the S-capacity of these melts.

P. Momme (✉) · C. Tegner
Geologisk Institut, Aarhus Universitet, 8000 Århus C,
Denmark
E-mail: peter@plan.aau.dk
Tel.: +45-9635-8384

C. K. Brooks
Geologisk Institut, Københavns Universitet,
Øster Voldgade 10, 1350 København K, Denmark

R. R. Keays
Victorian Institute of Earth and Planetary Sciences,
School of Geosciences, Monash University,
P.O. Box 28E, 3800 Victoria, Australia

Present address: P. Momme
Department of Development and Planning, Aalborg University,
Fibigerstraede 13, 9220 Aalborg OE, Denmark

Introduction

Some of the world's largest Ni–Cu–PGE deposits are associated with continental flood basalts (CFB) such as the Siberian Traps that have relatively high platinum-group elements (PGE) contents (Brügmann et al. 1993; Lightfoot and Keays 2005). The high PGE contents of these basalts as well as those of East Greenland (Momme et al. 2002) pose a problem because the lithophile elements indicate that their primary melts were formed by low to moderate degrees of partial melting while the chalcophile elements suggest very high degrees of mantle melting. Traditional mantle melting models indicate that the mean degree of partial melting, F, required for PGE-undepleted magmas to form is around 20–25% (Fryer and Greenough 1992; Keays 1995; Barnes and Maier 1999). These estimates are based on assumptions of sulphide content of the mantle and the amount of sulphide dissolved in the extracted partial melt. Komatiites are examples of PGE-undepleted magmas that are believed to originate from very high degrees of mantle melting (Zhou 1994; Keays 1995). In the case of CFB volcanism, however, inference from the incompatible lithophile trace elements such as the REE indicates that F is restricted to some 5–15% due to the presence of thick non-melting continental lithosphere capping the top portion of the melting column (Ellam

1992; Fram and Lesher 1993; Tegner et al. 1998a). Rare earth-element modelling of the East Greenland flood basalts presented in Tegner et al. (1998a) assumes partial melting of slightly depleted primitive mantle in a triangular melting regime (or 'corner flow' model; Langmuir et al. 1992; Fram and Lesher 1993) and the mean degrees of partial melting are indicated to be in the range 3–9%. If the inference about low F is correct for continental flood basalts, the PGE-rich nature (up to 25 ppb Pd, Momme et al. 2002) of the East Greenland flood basalts cannot be explained by the traditional melting models.

In this study we elaborate on PGE and REE data for the high- and low-Ti suites from the CFB sequence in central East Greenland published by Tegner et al. (1998a) and Momme et al. (2002). New forward models of mantle melting of the PGE is presented and combined with existing REE models to approximate the formation of PGE-rich, tholeiitic flood basalts. In contrast to other CFB sequences such as the Siberian Traps that exhibit significant crustal contamination (Lightfoot et al. 1994; Lightfoot and Keays 2005), the East Greenland Plateau Lava basalts show little or no signs of crustal contamination (< 5%, Larsen et al. 1989; Tegner et al. 1998a; Peate and Stecher 2003; Andreasen et al. 2004) and hence La, Sm, Cu and Pd concentrations may reflect mantle melting processes and subsequent fractional crystallisation. We propose here a scenario for the mantle melting conditions that reconciles the inferences from rare earth elements and platinum group elements. The role of melting hot, heterogeneous plume mantle during continental rifting in the formation of PGE-rich, S-undersaturated basalt as a prerequisite for Skaergaard-type PGE mineralisations is discussed. Finally, we evaluate the geodynamic implications for melting and plumbing systems during continental breakup from the contrasting mantle melting conditions implied by the forward models for the high- and low-Ti suites.

The East Greenland continental flood basalt province

Geological background

The East Greenland continental flood basalt province (Fig. 1) consists of the Lower Lavas (~2 km), the Plateau Lavas (> 5 km) and the uppermost Igtertiva formation and associated mafic intrusions emplaced mainly in three magmatic episodes at ~62–59, ~57–54 and ~50–47 Ma, respectively (Tegner et al. 1998b). The basalts exposed along the Blosseville Coast represent the largest onshore sequence in the Palaeogene North Atlantic large igneous province and the volume of magma formed in the region during continental breakup is estimated to be 6.6×10^6 km^3 (Head and Coffin 1997). The Plateau Lava sequence comprises more than 300 flow units and has a total thickness in excess of 6 km in the coastal area (Pedersen et al. 1997). From top to bottom, the flows are subdivided into the Skrænterne Formation, the Rømer Fjord Formation, the Geikie

Plateau Formation and the lowermost Milne Land Formation (Fig. 1). The tholeiitic Plateau Lavas are the subject of this paper and consist of three magmatic suites, viz: the low-Ti, high-Ti and very high-Ti suites which were extruded synchronously during the early stages of continental breakup at ~55 Ma (Pedersen et al. 1997; Tegner et al. 1998a, b). The low- and high-Ti suites constitute ~98% of the lava flows. The very high-Ti suite is very differentiated (< 6.6 wt% MgO) and it is not considered possible to estimate a primary magma composition for this suite. This paper therefore deals only with modelling of mantle melting of the low- and high-Ti suites.

In contrast to the continental high-Ti suite, the low-Ti suite is absent in inland areas and the number of flows increase towards the coast (Pedersen et al. 1997; Tegner et al. 1998a). The low-Ti suite is only present within the lower volcanic succession (Milne Land and Geikie Plateau Formations, Fig. 1). Although the high- and low-Ti suites are interbedded in the lower volcanic succession, Tegner et al. (1998a) demonstrated that the two magma types never mixed and therefore concluded that the two suites originated from two rift and plumbing systems that were concurrent but physically completely separate. The thicknesses of the lower volcanic succession are approximately the same across the exposed flood basalt region and eruption sites are evenly distributed (Pedersen et al. 1997). In contrast, the high-Ti suite that makes up the Rømer Fjord and Skrænterne formations are considerably thinner in the inland areas compared to the coastal areas and imply a shift of eruption sites towards the current coast line (Pedersen et al. 1997). For the lower volcanic succession, Tegner et al. (1998a) therefore suggested that the high-Ti suite formed below relatively thick, continental lithosphere and erupted in the inland rift systems while the low-Ti suite originated in a nascent oceanic rift located at the time to the east of the present coast line.

Previous geochemical studies

The high-Ti suite of the CFB magmas was sourced in a continental rift zone above the Palaeogene Icelandic mantle plume with relatively low to intermediate degrees of melting ($La_N/Sm_N > 1$; N denotes chondrite normalised) of asthenospheric material beneath thick non-melting lithosphere (Tegner et al. 1998a). Numerical approximation of REE in the high-Ti suite assuming melting in a spreading related, triangular, melting regime gave estimates of degrees of partial melting ranging between 3 and 9% (Tegner et al. 1998a). The low-Ti suite is depleted in LREE with $(La/Sm)_N$ of ~0.65. The low-Ti suite has $(Dy/Yb)_N$ of ~1 in contrast to the high-Ti suite with $(Dy/Yb)_N$ ~1.4 (Tegner et al. 1998a). The elevated $(Dy/Yb)_N$ of the high-Ti suite has been approximated to reflect melting of a source that includes garnet- and spinel-bearing residual mantle at depths between ~105 km (~35 kbar) and 50 km (~16 kbar) (Tegner et al. 1998).
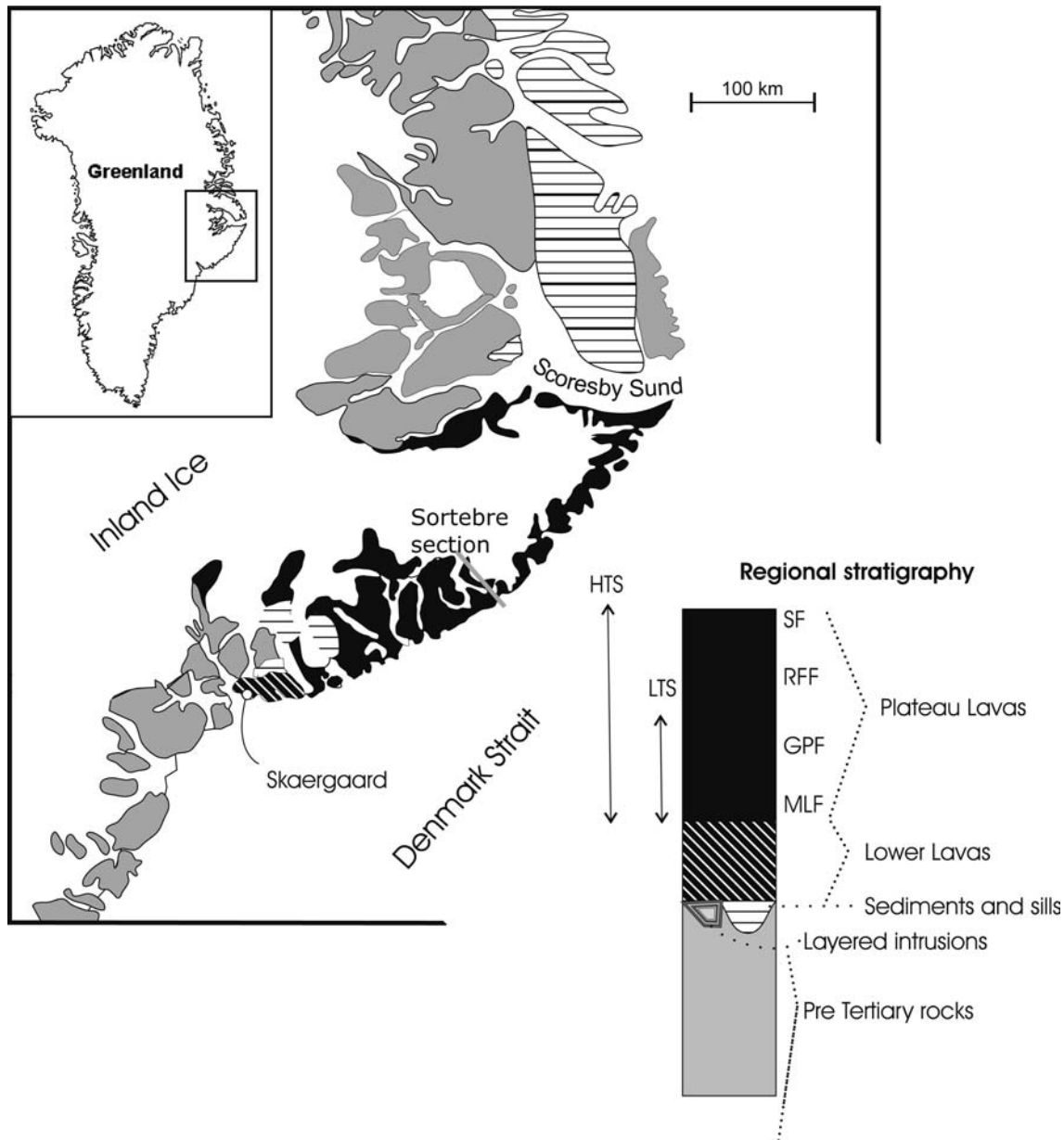
Fig. 1 Map of central East Greenland with a simplified regional stratigraphic column. *HTS* high-Ti suite, *LTS* low-Ti suite, *MLF* Milne Land Formation, *GPF* Geikie Plateau Formation, *RFF* Rømer Fjord Formation, *SF* Skrænterne Formation

In contrast, the low-Ti suite formed entirely within spinel-bearing mantle that is shallower than ∼ 60 km. In terms of Sr, Nd and Pb isotopes, the low-Ti suite resembles depleted Northeast Atlantic MORB while the high-Ti suite originated from a slightly more enriched source (Peate and Stecher 2003). Both the high- and low-Ti suites fall within the isotopic fields defined for Iceland and implies that their sources were part of the Iceland mantle plume (Peate and Stecher 2003).

Momme et al. (2002) showed that the Pd, Cu and La contents of both the high- and low-Ti suites increased with differentiation (Fig. 2) and concluded that, even though the most differentiated magmas of the high-Ti suite represents ∼60% fractional crystallization, these magmas did not reach S-saturation. The Cu/Pd ratios of the high-Ti suite (12,000–33,000) are dissimilar to mantle values (∼1,000–10,000) and may result from melting processes since both Cu and Pd behave incompatibly with *D*-values of ∼0.01 during silicate and oxide fractionation under S-undersaturated conditions (Momme et al. 2002). It cannot be ruled out that the high-Ti suite interacted with sulphides in the magma conduit, which could have elevated the Cu/Pd ratio, but the good correlation between Cu, Pd, La and Mg number (Fig. 2) shows that such interaction was limited (Momme et al. 2002). In contrast, the low-Ti samples have Cu/Pd ratios between 9,000 and 18,000 with an average of 12,000 which is close to mantle values. This suite of lavas also
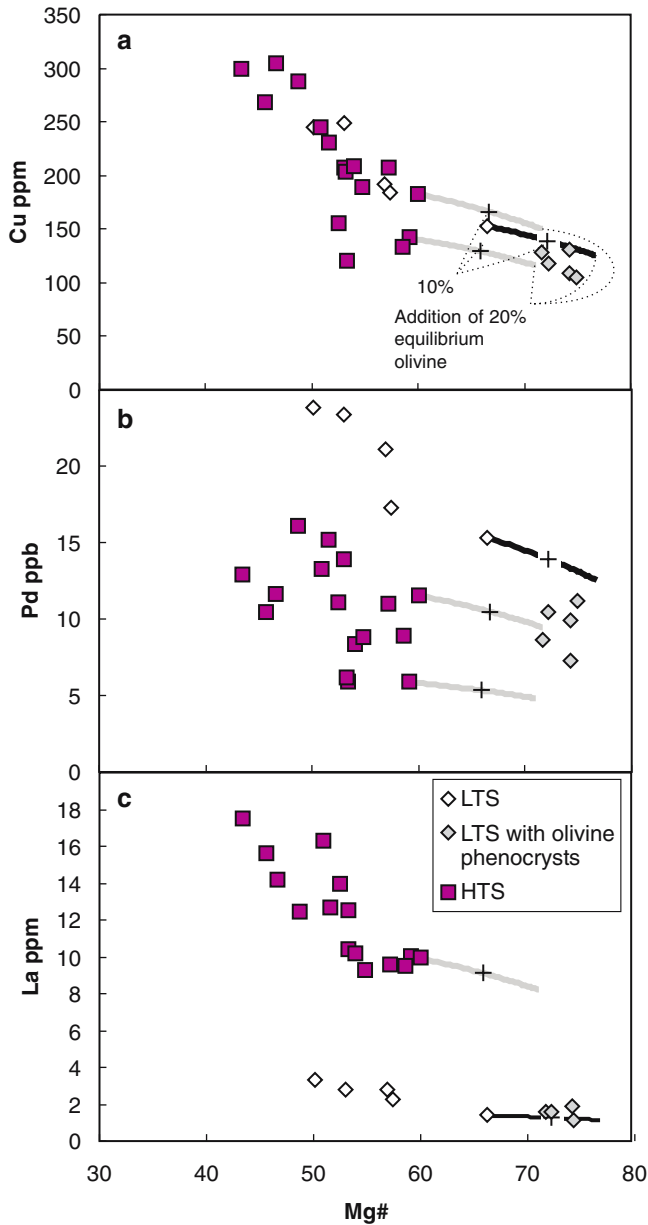
Fig. 2 Copper, Pd and La against Mg number. *HTS* High-Ti suite, *LTS* low-Ti suite. Both the high-Ti suite and low-Ti suite samples show increasing concentrations of the three elements with decreasing Mg number. The compositional effects of up 20% addition of equilibrium olivine has been calculated for two high-Ti suite samples (*grey lines*) and for one low-Ti suite sample (*black line*) using a $K_D^{Mg-Fe} = 0.30$ and the following melt-olivine partition coefficients La = 0.00003, Cu = 0.0001 and Pd = 0.0001. Tickmarks (+) on olivine addition curves indicate points of 10% olivine addition. Olivine addition trends have been based on two high-Ti suite due to compositional variation in the least evolved samples

differentiated under S-undersaturated conditions where Cu and Pd concentrations increased from 105 to 246 ppm and from 7 to 24 ppb, respectively. Isotopes and trace element compositions of both the high- and low-Ti suites show that contamination due to crustal assimilation was very restricted (Tegner et al. 1998a; Peate and Stecher 2003; Andreasen et al. 2004).

Generic mantle melting model

Copper and PGE

In a general mantle melting model presented in Fig. 3, it is assumed that the mantle contains 250 ppm S, the primary magma S-solubility is 1,000 ppm S (Mathez 1976) and that the mantle melts 1% per kb decompression (McKenzie and Bickle 1988; Langmuir et al. 1992). Equilibrium distribution of metals between mantle residuum and partial melt is calculated in 1% increments using sets of equations that consider mass-balance and sulphide–silicate partition coefficients. Partition coefficients and starting composition used for modelling the chalcophile elements here are presented in Table 1. Compatibility of Pd, Pt and Ir in mantle sulphides during mantle melting has been modelled assuming sulphide melt–silicate melt partition coefficients of 40,000 for all three elements, whereas sulphide melt–silicate melt partition coefficient for Cu was set to 1000 (Peach et al. 1994). Additionally, Ir compatibility in the non-sulphide residuum (silicates, alloys, spinel) has been modelled using bulk partition coefficient of ten decreasing linearly to five between 1 and 25% melting, respectively (Barnes and Maier 1999).

Modelling of PGE in magmas during mantle partial melting has traditionally been based on batch-melting of a columnar (cylindrical) melting regime (Keays 1995; Barnes and Maier 1999). This model assumes that the mantle source melts uniformly in the entire melting regime and as a consequence, these magmas extract all the sulphide-hosted PGE from the mantle source once sulphide is exhausted and therefore produce magmas with relatively high PGE-concentrations in high-*F* melts. In the columnar model, the mantle sulphide component is exhausted at *F* equal to ~25% and Cu, Pd and Pt reach their maximum concentrations at this stage. Partial melting beyond 25% only dilutes the concentrations of these chalcophile elements (Fig. 3b). Iridium, on the other hand, is also hosted by non-sulphide mantle phases, and the compatible behaviour leads to steady increasing concentrations during progressive partial melting also beyond 25% (Fig. 3). The Cu/Pd ratio of melts formed by less than 25% partial melting is higher than 100,000, because Pd is much more efficiently retained in the residual mantle sulphides (Fig. 3b). When *F* exceeds 25%, Cu/Pd drops to the mantle value around 6,000 resulting from total release of the mantle's inventory of Pd and Cu into the partial melt.

The triangular melting regime model is thought to be an appropriate approximation of melting beneath spreading ridges (Langmuir et al. 1992; Momme et al. 2003) and it assumes near-fractional melting in 1% melting steps (Rehkämper et al. 1999; Momme et al. 2003). The triangular melting regime model assumes perfect corner flow (Langmuir et al. 1992), where initial melting takes place when the mantle crosses the solidus and as long as the mantle upwells vertically the degree of
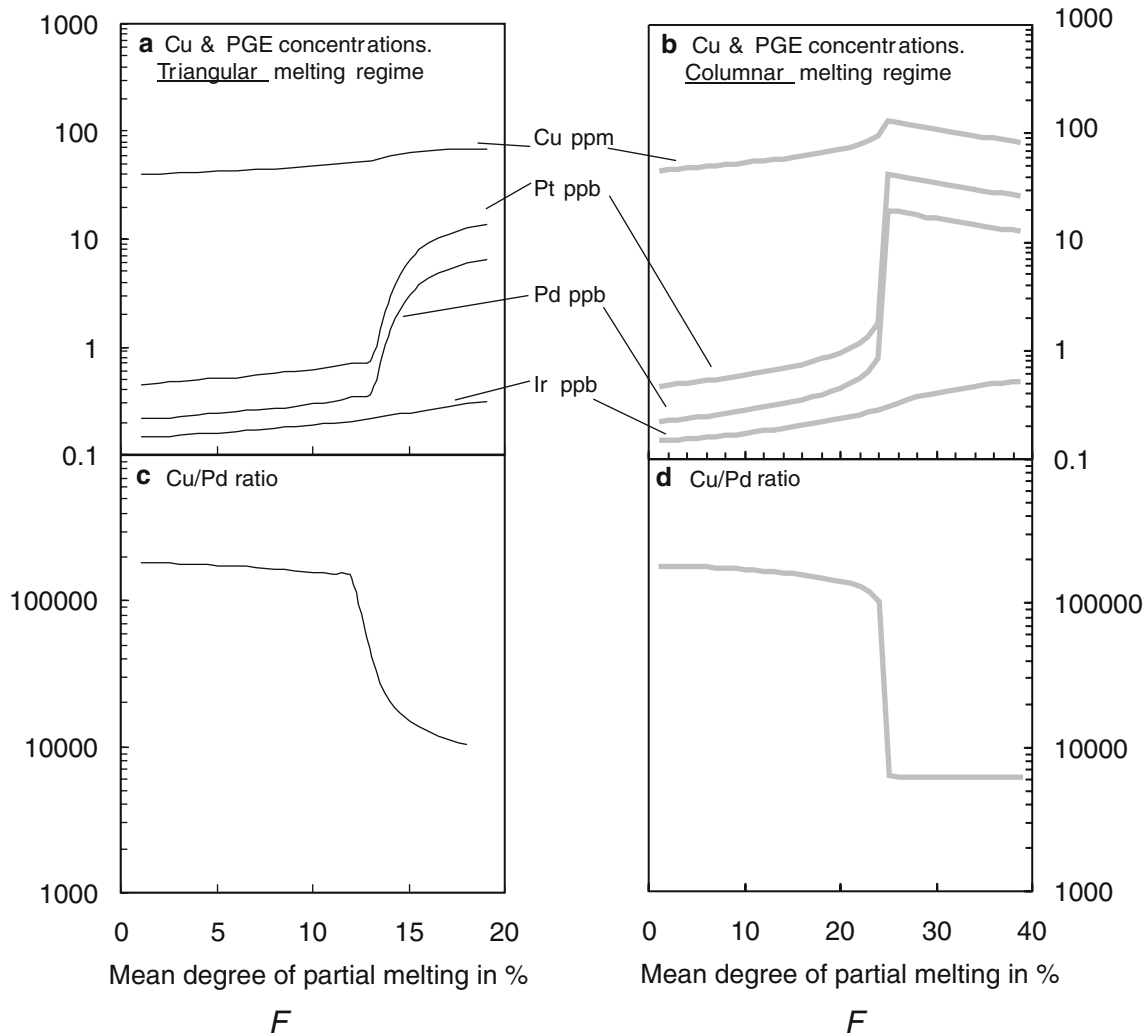
Fig. 3 The figure shows calculated general models of Cu, Pd, Pt and Ir concentrations in mantle derived melts. The modelling assumes a primitive mantle starting composition (4.4 ppb Pd, 4.4 ppb Pt, 9.2 ppb Pt, 28 ppm Cu and 250 ppm S) and a S-capacity of the partial melt of 1,000 ppm S. **a** Concentrations in melts derived from a triangular melting regime. **b** Concentrations in melts derived from a columnar melting regime. **c** and **d** Copper/Pd ratios of melts derived from triangular and columnar melting regimes, respectively

partial melting increases with vertical displacement. Following the general principles of Langmuir et al. (1992), low degree melts form in the distal and lowest parts of the triangular melting regime. Such low-F magmas are S-saturated at source, with low PGE-concentrations and high Cu/Pd > 100,000 (Fig. 3a). The highest degrees of partial melting occur in the top of the triangle and will most likely exhaust mantle sulphides and generate PGE-rich magmas with low Cu/Pd < 100,000 (Rehkämper et al. 1999; Momme et al. 2003). In the case of efficient collection of distal and central melt batches (efficient melt pooling), the aggregated

Table 1 Sulphide–silicate the partition coefficients used for modelling mantle melting and the initial mantle source concentrations of Cu, Pd, Pt and Ir

	Cu	Pd	Pt	Ir
Part. coefficients				
Sulphide–silicate melt	1,000	40,000	40,000	40,000
Silicate–silicate melt	0.001	0.001	0.001	10–5[a]
Initial concentration in source[b]	28 ppm	4.4 ppb	9.2 ppb	4.4 ppb

[a]Decreasing linearly from 10 to 5 between 1 and 25% partial melting
[b]From Barnes et al. (1988)

melts will have moderately-high PGE-concentrations of 0.3–7 ppb Pd and Cu/Pd ratios of 10,000–140,000 at F $\sim$11–20 % (Fig. 3).

Rare earth elements

The modelling of REE concentrations in partial melts presented here is taken from (Tegner et al. 1998a). It simulates forward modelling of adiabatic decompressional melting assuming 1% melting per kb (0.1 GPa) decompression similar to the model used for PGE modelling. The transition from garnet to spinel lithology is approximated as a linear function between 25 and 20 kb and the initial solid mode of olivine:opx:cpx:garnet is 55:15:20:10 (Lesher and Baker 1997). The initial mantle composition is assumed to be primitive mantle (Sun and McDonough 1989) depleted by 0.5% melting in the spinel stability regime.

During increasing amounts of mantle melting, the most incompatible element, La, yields upward concave evolution curves in both the columnar and triangular melting regime models (Fig. 4a, b). In general, the differences between the columnar and triangular melting models, as with the above models for the chalcophile elements, relates to the mixing of high degree melts with low degree melts in the triangular melting regime model. Since the low degree melts are so enriched in the incompatible lithophile elements, the triangular melting regime magmas are enriched over columnar melting regime-derived melts in such elements at the same mean degree of melting, F (Fig. 4), but the overall shape of the melting curves from the two models are similar.
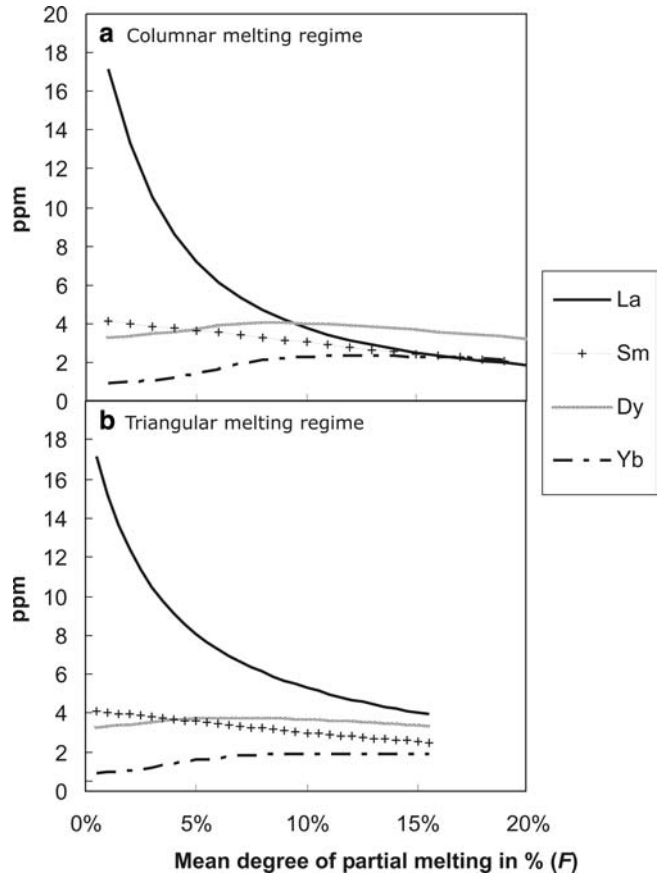
Fig. 4 Modelling REE in mantle derived melts using the model of Tegner et al. (1998a). **a** Columnar melting regime. **b** Triangular melting regime. The most incompatible REE is La and Dy and Yb are the most sensitive to retention in garnet

Specific mantle melting models for East Greenland lavas

Estimation of primary magma compositions

To model mantle melting, it is necessary first to estimate the compositions of the primary magmas which fractionated to form the high-Ti and low-Ti suites. Adapting the techniques of Fram and Lesher (1997) and Korenaga and Kelemen (2000), it will be assumed that olivine was the only fractionating phase involved in the modification of the primary magmas, that the primary magmas had a Mg# (defined as molar Mg/Mg + Fe) of $\sim$69–71 or that the forsterite (Fo) and Ni contents of the residual mantle olivine were 0.88–0.91 and 3,500 ppm, respectively. The techniques involve the addition of olivine in 0.5% steps to the most primitive melt compositions until either the forsterite or the Ni content of the equilibrium olivine equals residual mantle olivine. The compositions for a limited suite of elements (MgO, FeO, Ni, Cu, Pd, Pt La, Sm, and Dy) are calculated. The results of adding olivine to two primitive high-Ti samples are shown as grey lines in Fig. 2 and the results for the most primitive and aphyric low-Ti suite sample is shown as black lines. The crosses give the results after the addition of 10% olivine

whereas the tails of the curves record the addition of 20% olivine.

The low-Ti suite requires addition of 8% equilibrium olivine to the most primitive sample before the olivine has 3,500 ppm Ni whereas addition of 11% olivine is required before the equilibrium olivine composition is Fo$_{90}$. So there is relatively good agreement between the two methods for the low-Ti suite indicating that 8–11% olivine has been removed from the primary magma to produce the most primitive low-Ti basalt observed. If 10% olivine crystallisation is assumed, the primary magma had 13.6 wt% MgO, 9.3 wt% FeO, 460 ppm Ni, 1.3 ppm La, 1.6 ppm Sm, 2.8 ppm Dy, 14 ppb Pd, 19 ppb Pt and 139 ppm Cu. The most primitive non-cumulative sample used as the starting point for this correction was not analysed for PGE, but since this series has a constant mantle-like Cu/Pd ratio of $\sim$10,000 (Momme et al. 2002), the Pd-concentration can be estimated to $\sim$15 ppb. With respect to most elements the calculated composition is broadly comparable to the group of primitive low-Ti samples which may be slightly olivine cumulative.

It is more complex to correct the least fractionated high-Ti suite sample for olivine fractionation since

lavas of this lineage have undergone complex differentiation processes including replenishment, tapping and fractionation (Larsen et al. 1989). If a primitive sample is corrected for 7% olivine fractionation, the equilibrium olivine contains 3,500 ppm Ni and the equilibrium liquid contains 11 wt% MgO, 12 wt% FeO and 330 ppm Ni. This melt is in equilibrium with Fo$_{86}$ olivine. If it is assumed that the primary magma was in equilibrium with Fo$_{88}$ olivine, correction for 13% olivine fractionation is required and the primary magma had in this case 13 wt% MgO, 12 wt% FeO, ~570 ppm Ni. This larger discrepancy between the two methods to estimate primary high-Ti suite magmas can result from several factors. The least fractionated high-Ti suite sample has 8.4 wt% MgO, and both field observations and petrography reveal plagioclase and clinopyroxene phenocrysts in addition to olivine. Korenaga and Kelemen (2000) only used samples with MgO > 8.5 wt% otherwise they found it possible that the sample had experienced poly-phase fractionation. If plagioclase fractionated prior to MgO reached ~8.4 wt% this could have increased incompatible elements and the Ni concentrations significantly. We conclude that the Fe-rich composition of the high-Ti suite reflects, in part, their highly differentiated state developed in RTF-magma chambers beneath the region during continental break up (Brooks et al. 1991), and that this may make it difficult to use a simple addition of equilibrium olivine to 8.4 wt% MgO magmas to gain insight about primary magma compositions. The two correction methods have therefore been averaged (Table 2) to yield a rough estimate for the primary high-Ti magma composition with ~12 wt% MgO, 9.3 wt% FeO (Mg number 66; in equilibrium with Fo:87 olivine), 458 ppm Ni, 9 ppm La, 4.4 ppm Sm, 4 ppm Dy, 7 ppb Pd and 150 ppm Cu.

The S content of the primary magmas can be estimated from the composition and differentiation history of the high and low-Ti suite. Since all samples have FeO > 10 wt%, the S-capacity of the magma can be estimated from the FeO content (Poulson and Ohmoto 1990) using the equation $\log X_S = -0.92 + 1.92 \log X_{FeO}$. Based on the measured Zr contents of each sample, the degree of fractional crystallization can be estimated. If the fraction of remaining melt is coupled to a calculated S-capacity of the sample, it is possible to depict the S-content at sulphide saturation as differentiation proceeds (Fig. 5). The most primitive high-Ti samples (10.0–10.3 wt% FeO) can dissolve 1,200–1,500 ppm S whereas the most evolved, iron-rich sample with 14.2 wt% FeO can dissolve ~2,800 ppm S. The low-Ti suite also shows an increase in S-capacity during differentiation from 1,200 to 2,200 ppm reflecting iron enrichment from 10 to 12.4 wt% FeO. It can be concluded that both the low and high-Ti suites would have no difficulty in keeping S in solution if the initial concentration was 900 ppm. So if an initial S-capacity of the partial melt in mantle melting models presented below is set to 900 ppm, it is still plausible that the melts remained S-undersaturated due to the significant FeO-increase during differentiation.

Results of forward modelling

We will now investigate whether different melting regimes may explain the observed differences in REE and PGE between the high- and low-Ti suites. It should be noted that in our modelling of Cu and PGE behaviour during melting, we assume the same mantle starting composition, primitive mantle depleted by 0.5% batch melting (Tegner et al. 1998a), but with different S contents. Although it has been shown that the source of low-Ti and high-Ti lavas had very different elemental and isotopic compositions (Tegner et al. 1998a; Peate and Stecher 2003), these differences are negligible in the Cu and PGE modelling. The concentration of Cu and PGE would not be affected by such a low-F depletion event since the amount of mantle sulphide would not be significantly changed, so with respect to Cu and PGE, the initial composition can be assumed to be primitive mantle (Pd 4.4 ppb, Pt 9.2, Ir 4.4 ppb, Cu 28 ppm; Barnes and Maier 1999).

The low incompatible element contents as well as the relatively high PGE contents of the low-Ti parent are all indicative of formation by high degrees of melting. The high PGE-contents indicate formation in a columnar melting regime by high degrees of melting (Fig. 6). The observed Cu and PGE concentrations in the low-Ti suite can be approximated if the mantle contains 180 ppm S, which is very close to 200–300 ppm S estimated for normal primitive mantle (McDonough and Sun 1995). It has previously been proposed that this suite formed by 15–25% partial melting similar to present-day North Atlantic MORB (Tegner et al. 1998a) and we conclude that modelling of Cu and PGE indicate degrees of melting around 18–20%. In conclusion, both REE and PGE modelling indicate formation of the low-Ti series primary magma by high degrees of melting of ~20%.

The attempt to approximate the high-Ti primary composition by using a *columnar* melting regime model fails. The elements taken into account here indicate formation by different mean degrees of melting ranging from 4 to 20% (Table 2). This Ti-rich suite of tholeiites has previously been recognised to be derived from an asthenospheric source by 3–9% melting in a spreading related, triangular melting regime (Tegner et al. 1998), and we intend investigate if the triangular melting regime model can reconcile the degree of melting obtained from modelling of Cu, PGE and REE.

The high-Ti suite has higher Cu/Pd ratios (15,000–35,000) than the mantle, which has a Cu/Pd ratio of ~10,000 (McDonough and Sun 1995). The high-Ti suite has Cu, REE and PGE-concentrations similar to melts formed in a triangular melting regime with F ranging from 5 to 7% from a relatively S-poor source with 100 ppm S (Fig. 6). If it is assumed that the source was richer in S, e.g., a normal 250 ppm S, it would not be

Table 2 The calculated range of concentrations of La, Sm, Dy, Yd, Cu, Ni and Pd when samples have been corrected for fractionation and the resulting average concentration which gives the estimated high-Ti and low-Ti primary magmas

	La	Sm	Dy	Yb	Cu	Ni	Pd (ppb)
Low-Ti series							
Concentration[a]	1–2	2	3–4	2	137–150	400–600	14–15
Calculated primary magma estimate[b]	1.3	1.6	2.8	2.0	139	460	14
Best-fit F^c (%)	20	20	20	20	20	18–19	19–20
High-Ti series							
Concentration[a]	9–10	4–5	3–5	2	120–170	300–700	5–11
Calculated primary magma estimate[b]	9.0	4.4	4.0	2.0	150	458	7
Best-fit F^c (%)	5–6	4–5	7–8	7–8	19–20	17–18	19–20

The calculated Low-Ti series parent is similar to melts formed by 18–20% partial melting in a columnar melting regime. Based on the elements in the High-Ti series parent and a columnar melting regime model, the various elements indicate formation by degrees of melting between 4 and 20% indicating that a columnar melting regime model is not a good approximation for the generation of this lava suite
[a]Calculated compositional range of melts after correction for fractionation
[b]The preferred calculated primary magma composition is the calculated average of the two fractionation correction methods (see text for details)
[c]The F-estimate that best approximates the calculated primary magma assuming a columnar melting regime and a source composition similar to primitive mantle depleted by 0.5% batch melting in the spinel stability field
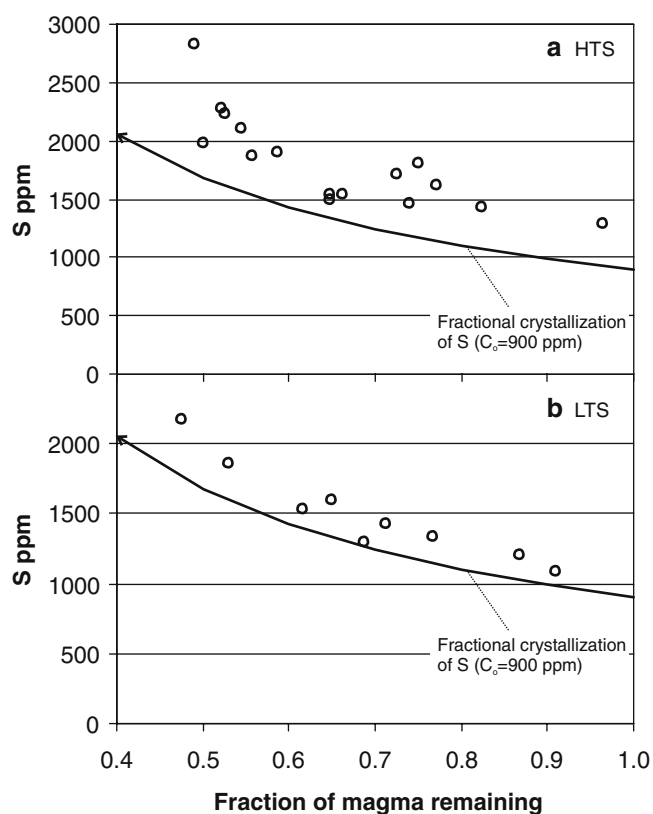
Fig. 5 Sulphur capacity of the melts versus degree of fractionation. The theoretical S-capacity of each sample is calculated using the Poulson and Ohmoto (1990) relation between FeO and S-capacity (*open circles*). It is assumed that $Fe_2O_3/FeO = 0.15$. Degree of fractionation, calculated for each sample, is derived by rearranging the Rayleigh fractionation equation and assuming an initial Zr concentration of 40 and 95 ppm for the low-Ti suite and high-Ti suite, respectively. The *solid line* in each diagram represents a model of fractional crystallisation of S using an initial S-content of both series of 900 ppm S. It can be concluded that both series could have fractionated under S-undersaturated conditions since the FeO-increase during fractionation causes an S-capacity increase of the melt at the same time as S-concentration builds up due to incompatible behaviour of S

possible to approximate the suitable high-Ti suite primary magma with ~150 ppm Cu and ~7 ppb Pd (Fig. 7). At the suitable Cu/Pd ratio, the chalcophile element concentrations would be far too low. There are several indicators from previously published reports that support the derivation of the high-Ti suite from a S-poor source. These lavas experienced more than ~60% fractional crystallization during which Cu and Pd concentrations increased, indicating massive potential for S-undersaturated fractionation during cooling (Momme et al. 2002). The Skaergaard Intrusion that formed from a high-Ti magma which crystallised ~75% prior to reaching S-saturation (Momme et al. 2002; Nielsen 2004). The most logical explanation for the very prolonged history of fractionation under S-undersaturated conditions is that the magmas were derived from S-poor sources.

It is clear that the Cu-PGE-REE concentrations of the high-Ti primary magma are best explained by formation in a triangular melting regime (Figs. 6, 8). A melt derived from a triangular melting regime by 6% partial melting is relatively rich in La and has intermediate Pd-concentrations (~6 ppb), which contrasts the suitable low-Ti suite primary magma, more La-poor, derived by $F = 19–20\%$ in a columnar melting regime.

Discussion

Heterogeneous S content of the Iceland mantle plume

A conclusion of the melting models is that the S-contents of the high-Ti suite source (100 ppm) had to be lower compared to relatively normal values (180 ppm) of the low-Ti suite source. The observed compositional variations can then be explained by melting in a columnar and triangular melting regime, respectively, followed by significant fractionation, equivalent to 60% fractional crystallisation, under S-undersaturated conditions
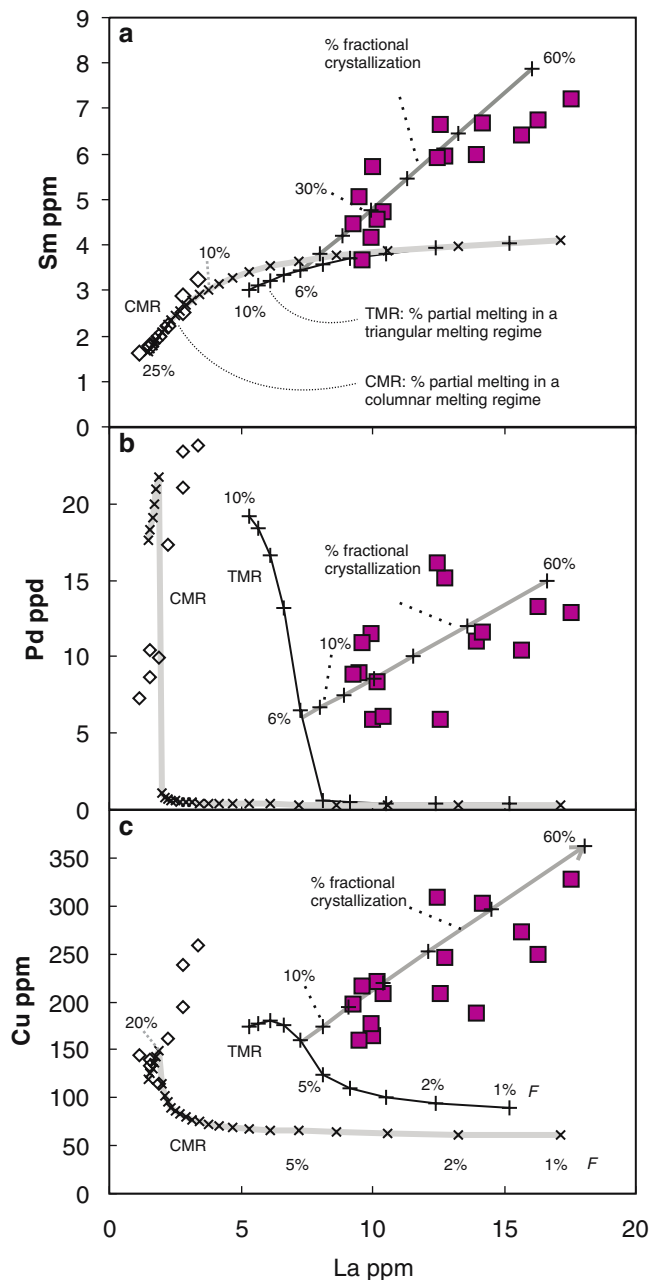
Fig. 6 Scattergrams of Sm, Pd and Cu versus La. *F* Mean degree of melting; *CMR* columnar melting regime; *TMR* triangular melting regime. The low-Ti suite and high-Ti suite samples are plotted along with columnar (F_{CMR}; 1–25% partial melting) and triangular (F_{TMR}; 1–10% partial melting) melting regime models. Fractional crystallisation modelling (0–60%) of a suitable high-Ti suite primary magma is shown in all diagrams. A suitable low-Ti suite primary magma is best approximated by ~20% melting in a columnar melting regime whereas a suitable primary high-Ti suite magma is best approximated by ~6% melting in a triangular melting regime

(Momme et al. 2002). The S content (~180 ppm) of the low-Ti suite source was very close to that of a normal MORB source (200–300 ppm S) (McDonough and Sun 1995), so with respect to this suite, REE and PGE modelling both indicate similar high degrees of melting

~20%. Even though the low-Ti suite has compositional similarities to MORB, these melts formed during initiation of oceanic spreading in the region, and are likely to represent the earliest melting product derived by initial upwelling into the zone of continental rupture. It is therefore likely that they were generated in a columnar melting regime by high degrees (~20%) of partial melting, as indicated by both their REE and PGE contents.

The explanation for the low S-contents of the high-Ti suite is less clear. A S-concentration of 100 ppm could be an original characteristic of the high-Ti source, or an originally normal 250 ppm S upper mantle source could have experienced removal of S (and/or addition of S-poor material). There is, of course, a possibility that the high-Ti suite source stems from the Paleogene Iceland plume and may represent a mantle reservoir emerging from great depth as suggested by many authors (Tegner et al. 1998; Peate and Stecher 2003). Support to this notion may be the fact that Holocene Icelandic tholeiites are also S-undersaturated (with MgO > 7 wt%; Momme et al. 2003) in contrast to a normal PGE-poor MORB-composition (Rehkämper et al. 1999). Hence, the S-poor source may be a long-lived feature within the Iceland plume. Numerical modelling of REE and PGE concentrations of primitive Hawaiian melts led Bennett et al. (2000) to suggest highly varying S-contents between 0 and 0.1 wt% sulphide (equivalent 0 to ~350 ppm S) in the mantle plume source beneath Hawaii. In conclusion, recent efforts to reconcile REE and PGE melting models indicate that mantle plume sources may host a range of compositional reservoirs with respect to S-contents, low S-sources *are* needed to reconcile modelling of PGE and REE compositions in both Hawaii and central East Greenland.

Role of adiabatic decompression and S-solubility

The depth of magma generation may have a significant bearing on the S-saturation status of the magmas. Underway from the melting zone to the surface, individual melt batches and aggregated melts are likely to experience adiabatic decompression. If the distance from source to surface is large, which is the case for continental flood basalts erupted through thick lithosphere, adiabatic ascent may drive magma to S-undersaturation even if it was S-saturated at source (Mavrogenes and O'Neill 1999). We suspect this plays an important role in continental flood basalt generation. The observed HREE-depletion in the East Greenland high-Ti suite has been modelled to reflect melt segregation for this suite at 15–25 kb (Tegner et al. 1998a). In this pressure interval, laboratory experiments suggest a S-capacity of synthetic basalt range from 750 (~25 kb) ppm to 1,250 (~15 kb) ppm S (Determined from Fig. 2 in Mavrogenes and O'Neill 1999). We therefore argue that continental flood basalts may become S-undersaturated simply as a function of high segregation pressure and adiabatic
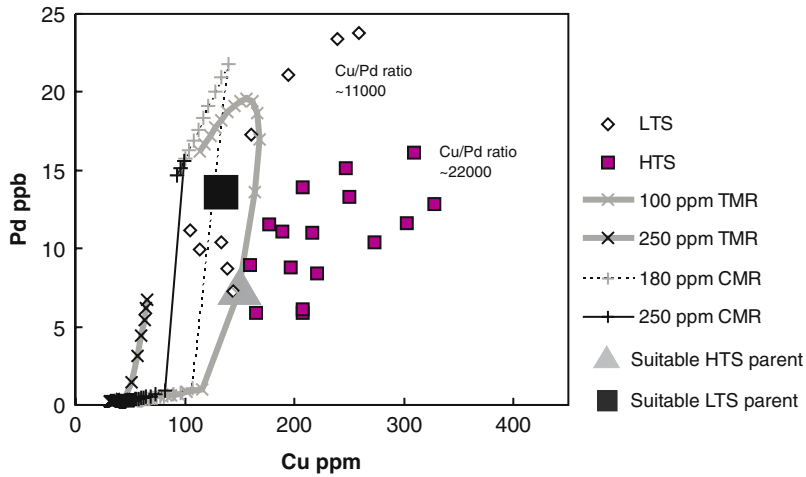
Fig. 7 A diagram showing Pd against Cu for the high-Ti suite and low-Ti suite samples. *CMR* columnar melting regime, *TMR* triangular melting regime. The suitable high-Ti suite (*HTS*) parent can be approximated by 6% melting of a source with 100 ppm S using a S-capacity of 1,000 ppm. If a normal S-content of the mantle is used, it is not possible to generate a suitable primary high-Ti suite magma (*grey triangle*). At the appropriate Cu/Pd ratio (~22,000) the concentrations would be far too low (~50 ppm Cu and 2 ppb Pd) and require much more than the allowed 15% olivine fractio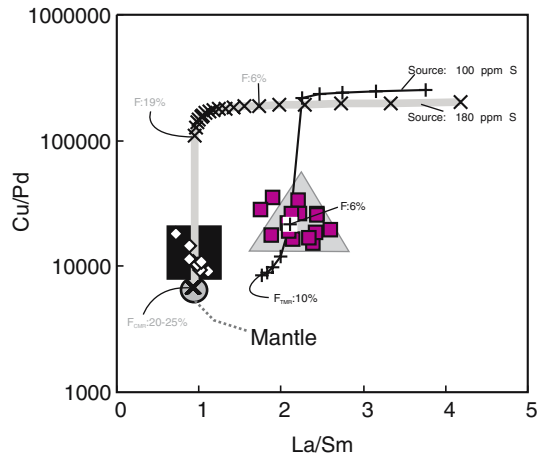nation (see text) before reaching the compositions of the most primitive (Cu and Pd-poor) high-Ti suite samples; in addition the required degrees of melting would be much higher ~16%. A suitable low-Ti suite (*LTS*) parent (*black square*) is compositionally similar to the least evolved low-Ti suite samples and can be approximated by 19–20% melting of a 180 ppm S source. A 'normal' 250 ppm S source would require higher degrees of melting ~25% to generate the suitable Cu/Pd ratio ~11,000 at which stage the Cu and Pd concentrations would be to low (80 ppm Cu and 7 ppb Pd) compared to the primary magma estimate (Table 2)

ascent. Mid-ocean ridge basalts are, on the other hand, typically S-saturated and PGE-poor (Barnes et al. 1988; Rehkämper et al. 1999). This is most likely because such basalts are generally extracted at low pressure beneath relatively thin lithosphere and thus does not experience the same increase in S-capacity due to adiabatic ascent. The fundamental difference in S-saturation status and PGE contents between MORB and the East Greenland continental flood basalts could therefore relate to the depth of segregation and possibly adiabatic ascent.

Implications for the geological development of the East Greenland volcanic rifted margin

The head of the Icelandic plume may have arrived beneath the North Atlantic lithosphere at ~62 Ma and the oceanic rift, which developed to the east of the current East Greenland coast, was stabilized at ~55 Ma (Storey et al. 1998; Tegner et al. 1998b). During this time, there must have been a period of dynamic interplay between the development of the oceanic rift, pre-existing crustal features such as the Caledonian suture zone, that potentially was a weak lineament in the crust, and upwelling, flattening and spreading of the plume head beneath the North Atlantic lithosphere. Continental rupture occurred at a stage close to or above the Geikie Plateau- and Rømer Fjord Formation boundary ~55 Ma (Larsen et al. 1989; Pedersen et al. 1997; Tegner et al. 1998a). The low-Ti suite flows in the studied profile were thus formed during initiation of oceanic spreading in the North Atlantic and not from a well-established

oceanic rift despite their MORB-like appearance (Larsen et al. 1999). They are probably the result of initial upwelling into an early precursor of an oceanic spreading centre. The absence of low-Ti basalts in the upper part of the Plateau Lava sequence could reflect the inability of these magmas to flow out of the oceanic rift zone as it matured further to the east of the present coast line.

Fig. 8 Cu/Pd versus La/Sm with East Greenland samples and mantle melting modelling. The *triangle* encircles most high-Ti suite samples that can be approximated by formation in a triangular melting regime by *F*~6%. The *black square* encircles the low-Ti suite samples which resembles melts formed from a columnar melting regime by *F*~19–20%. This diagram may be efficient to discriminate between magmas formed in different melting regimes
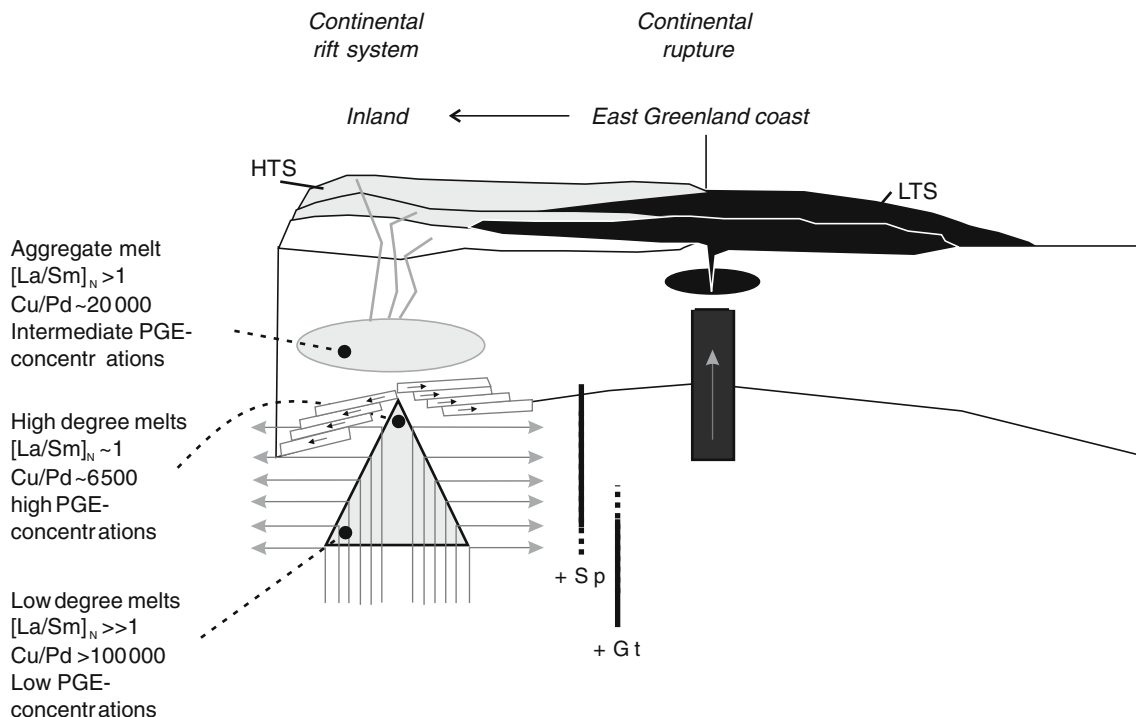
Fig. 9 Modelling REE and PGE during mantle melting indicates that the interlayered high-Ti suite and low-Ti suite formed in different melting regimes where the high-Ti suite segregated from triangular melting regime in the garnet zone, in contrast to the low-Ti suite which segregated at shallower level from a columnar melting regime by initial upwelling into the zone where continental break up were to occur later

The relatively steep REE patterns of the high-Ti suite are likely to reflect melt segregation at depth beneath thick lithosphere, partly in the garnet stability field. As noted by Tegner et al. (1998a), the potential temperature of the high-Ti suite mantle source is 1,500–1,420°C, which is lower than estimates of the present-day Iceland plume >1,500°C (Schilling 1991; Langmuir et al. 1992; Wolfe et al. 1997) but higher than estimates for modern ambient mantle 1,280–1,310°C (McKenzie and Bickle 1988; White and McKenzie 1995).

To map out the events leading to the observed extreme degree of S-undersaturated differentiation several pivotal factors have been outlined above. The REE modelling indicates a deep (high-Ti suite) and a shallow (low-Ti suite) melting regime, respectively (Tegner et al. 1998), where the deep melting requires abnormally hot mantle.

The high-Ti suite formed from a mantle source with elevated temperature, most likely the mantle plume itself. We attribute the triangular melting regime to melting of plume head material that had spread out beneath the lithosphere, causing thinning and local rifting of the continental lithosphere below what is today the inland area of the flood basalt outcrops (Fig. 9). This model is supported by the development of north–south striking rift basins in the inland areas in which sediments and the Lower Lavas were deposited prior to flood volcanism (Nielsen et al. 1981; Ukstins Peate et al. 2003). However, the final splitting of the continent occurred further to the east and the initiation of the nascent

spreading ridge is in our view represented by the low-Ti suite within the lower volcanic portion of Sortebre profile (Tegner et al. 1998; Larsen et al. 1999). Hence, the formation of the low-Ti suite is interpreted as a transient phenomenon developed during continental breakup which allowed rapid ascent of mantle into a steep-sided zone of rupture (Fig. 9). The triangular melting model suggested for the upper volcanic portion eventually evolved into full-scale oceanic sea-floor spreading forming the Greenland-Iceland Rise (Holbrook et al. 2001).

Conclusions

The compositions of the primary magmas to the low and high-Ti suites of East Greenland have been estimated by correcting for olivine fractionation prior to the formation of the most primitive representatives of each of these suites. The S, Cu and PGE concentrations of the primary magmas have then been modelled using both the triangular and columnar melting regime models.

The low-Ti suite has relatively high concentrations of PGEs and the estimated primary magma contains 13.6 wt% MgO, 9.3 wt% FeO, 460 ppm Ni, 1.3 ppm La, 1.6 ppm Sm, 2.8 ppm Dy, 14 ppb Pd, 19 ppb Pt and 139 ppm Cu. This composition is similar to a calculated melt composition formed by 19–20% partial melting of a slightly depleted mantle with 180 ppm S in a columnar melting regime.

A suitable high-Ti primary magma was estimated to ~12 wt% MgO, 9.3 wt% FeO, 458 ppm Ni, 9 ppm La, 4.4 ppm Sm, 4 ppm Dy, 7 ppb Pd and 150 ppm Cu, and can be approximated by near-fractional melting in a triangular melting regime with a mean degree of partial melting of ~5–7%. Modelling requires the high-Ti suite source had ~100 ppm S which is less than the estimates of primitive mantle (250 ppm S). The prolonged S-*undersaturated* differentiation history of these basalts and comagmatic intrusions such as the Skaergaard Intrusion also indicate a S-poor source.

Melting of a S-poor (~100 ppm), hot, asthenospheric mantle source beneath thick rifting continental lithosphere, and adiabatic decompression during magma ascent can lead to S-undersaturated differentiation of a basalt suite with Cu/Pd ratios 12,000–30,000. This is most probably a mantle plume source.

Adiabatic decompression experienced by the magma *en route* to the surface can drive the primary magmas to a state of S-undersaturation.

Iron-enrichment during magmatic differentiation is able to keep an initial concentration of 900 ppm S in solution during significant amounts of fractional crystallization in both magmatic suites.

Mantle melting models and evidence from East Greenland continental flood basalts indicate that S-undersaturated mantle-derived magmas do not necessarily have mantle-like Cu/Pd since Cu/Pd ratios can reflect mantle melting processes.

The integrated REE & PGE approach developed here splices the inferences from PGE and REE on mantle melting and may explain observed geochemical features of the low-Ti series and high-Ti series of the East Greenland Plateau Basalt lava types by melt generation in both columnar and triangular melting regimes.

We interpret the tectonic setting of the high-Ti suite to be an initial episode of lithospheric thinning and rifting above the head of the Iceland plume. The tectonic forces imposed by continental splitting lead to a relocation of the rift to the East of the present coastline where mantle upwelling into the continental rupture led to formation of the low-Ti suite.

References

Andreasen R, Peate D, Brooks C (2004) Magma plumbing systems in large igneous provinces: inferences from cyclical variations in Palaeogene East Greenland basalts. Contrib Mineral Petrol 147:438–452

Barnes S-J, Boyd R, Korneliussen A, Nilsson L-P, Often M, Pedersen RB, Robins B (1988) The use of mantle normalization and metal ratios in discrimination between the effects of partial melting, crystal fractionation and sulphide segregation on platinum-group elements, gold, nickel and copper: examples from Norway. In: Prichard HM, Potts PJ, Bowles JFW, Cribb SJ (eds) Geo-platinum symposium volume. Elsevier, London, pp 113–143

Barnes S-J, Maier WD (1999) The fractionation of Ni, Cu and the noble metals in silicate and sulphide liquids. In: Keays RR, Lesher CM, Lightfoot PC, Farrow CEG (eds) Dynamic processes in magmatic ore deposits and their application in mineral exploration. Geological Association of Canada, Short Course volume 13, pp 69–106

Bennett VC, Norman MD, Garcia MO (2000) Rhenium and platinum group element abundances correlated with mantle source components in Hawaiian picrites: sulphides in the plume. Earth Planet Sci Lett 183:513–526

Brooks CK, Larsen LM, Nielsen TFD (1991) Importance of iron-rich tholeiitic magmas at divergent plate margins. Geology 19:269–272

Brügmann GE, Naldrett AJ, Asif M, Lightfoot PC, Gorbachev NS, Fedorenko VA (1993) Siderophile and chalcophile metals as tracers of the evolution of the Siberian Trap in the Noril'sk region, Russia. Geochim Cosmochim Acta 57:2001–2018

Ellam RM (1992) Lithospheric thickness as a control on basalt geochemistry. Geology 20:153–156

Fram MS, Lesher CE (1993) Geochemical constraints on mantle melting during creation of the North Atlantic basin. Nature 363:7112–715

Fram MS, Lesher CE (1997) Generation of polybaric differentiation of East Greenland early Tertiary flood basalts. J Petrol 38:231–275

Fryer BJ, Greenough JD (1992) Evidence for mantle heterogeneity from platinum-group-element abundances in Indian Ocean basalts. Can J Earth Sci 29:2329–2340

Head JW, Coffin MF (1997) Large igneous provinces: a planetary perspective. In: Mahoney JJ, Coffin MF (eds) Large igneous provinces: continental, oceanic, and planetary flood volcanism. Geophysical Monograph, pp 411–438

Holbrook WS, Larsen HC, Korenaga J, Dahl-Jensen T, Reid I, Kent G, Hopper J, Kelemen P, Bernstein S, Detrick R, Lizarralde D (2001) Mantle thermal structure and active upwelling during continental breakup in the North Atlantic. Earth Planet Sci Lett 190:251–266

Keays RR (1995) The role of komatiitic magmatism and S-saturation in the formation of ore deposits. Lithos 34:1–18

Korenaga J, Kelemen PB (2000) Major element heterogeneity in the mantle source of the North Atlantic igneous province. Earth Planet Sci Lett 184:251–268

Langmuir CH, Klein EM, Plank T (1992) Petrological systematics of mid-ocean ridge basalts: constraints on melt generation beneath ocean ridges. In: Morgan JP, Blackman DK, Sinton JM (eds) Mantle flow and melt generation at mid-ocean ridges. Geophysical monographs 71, pp 183–275

Larsen LM, Waagstein R, Pedersen AK, Storey M (1999) Trans-Atlantic correlation of the Paleogene volcanic successions in the Faroe Islands and East Greenland. J Geol Soc Lond 156:1081–1095

Larsen LM, Watt WS, Watt M (1989) Geology and petrology of the Lower Tertiary plateau basalts of the Scoresby Sund region, East Greenland. Geological Survey of Greenland Bulletin, 157. Geological Survey of Greenland, Copenhagen, 162 pp

Lesher C, Baker M (1997) Near-solidus phase relations of mantle peridotite at 3.6–5 GPa. AGU Fall Meeting. San Francisco. Eos, Transactions, AGU 78:46, F812

Lightfoot PC, Keays R (2005) Siderophile and chalcophile metal variations in flood basalts from the Siberian Trap, Noril'sk Region: implications for the origin of the Ni–Cu–PGE sulfide ores. Econ Geol (in press) available on line

Lightfoot PC, Naldrett AJ, Gorbachev NS, Fedorenko VA, Hawkesworth CJ, Hergt J, Doherty W (1994) Chemostratig-

raphy of Siberian Trap lavas, Noril'sk District: implications for the source of flood basalt magmas and their associated Ni–Cu mineralization. In: Lightfoot PC, Naldrett AJ (eds) Proceedings of the Sudbury, Noril'sk symposium, pp 283–312

Mathez EA (1976) Sulfur solubility and magmatic sulphides in submarine basalt glass. J Geophys Res 81(23):4269–4276

Mavrogenes JA, O'Neill HSC (1999) The relative effects of pressure, temperature and oxygen fugacity on the solubility of sulfide in mafic magmas. Geochim Cosmochim Acta 63(7/8):1173–1180

McDonough WF, Sun S-S (1995) The composition of the Earth. Chem Geol 120:223–253

McKenzie D, Bickle MJ (1988) The volume and composition of melt generated by extension of the lithosphere. J Petrol 29:625–679

Momme P, Oskarsson N, Keays RR (2003) Platinum-group elements in the Icelandic rift system: melting processes and mantle sources beneath Iceland. Chem Geol 196:209–234

Momme P, Tegner C, Brooks CK, Keays RR (2002) The behaviour of platinum-group elements in basalts from the East Greenland Rifted Margin. Contrib Mineral Petrol 143:133–153

Nielsen T (2004) The shape and volume of the skaergaard intrusion, Greenland: implications for mass balance and bulk composition. J Petrol 45:507–530

Nielsen TFD, Soper NJ, Brooks CK, Faller AM, Higgins AC, Matthews DW (1981) The pre-basaltic sediments and the lower basalts at Kangerdlugssuaq: their stratigraphy, lithology, paleomagnetism and petrology, vol 6. Meddelser om Grønland, Geoscience, p 28

Peach CL, Mathez EA, Keays RR, Reeves SJ (1994) Experimentally determined sulfide melt–silicate melt partition coefficients for iridium and palladium. Chem Geol 117:361–377

Peate D, Stecher O (2003) Pb isotope evidence for contributions from different Iceland mantle components to Palaeogene East Greenland flood basalts. Lithos 67:39–52

Pedersen AK, Watt M, Watt WS, Larsen LM (1997) Structure and stratigraphy of the Early Tertiary basalts of the Blosseville Kyst, East Greenland. J Geol Soc Lond 154:565–570

Poulson S, Ohmoto H (1990) An evaluation of the solubility of sulfide sulfur in silicate melts from experimental data and natural samples. Chem Geol 85:57–75

Rehkämper M, Halliday AN, Fitton JG, Lee D-C, Wieneke M, Arndt NT (1999) Ir, Ru, Pt and Pd in basalts and komatiites: new constraints for the geochemical behaviour of the platinum-group elements in the mantle. Geochim Cosmochim Acta 63(22):3915–3934

Schilling J-G (1991) Fluxes and excess temperatures of mantle plumes inferred from their interaction with migrating mid-oceanic ridges. Nature 352:397–403

Storey M, Duncan RA, Pedersen AK, Larsen LM, Larsen HC (1998) 40Ar/39Ar geochronology West Greenland Tertiary volcanic province. Earth Planet Sci Lett 160: 569–586

Sun S-s, McDonough WF (1989) Chemical and isotopic systematics of oceanic basalts: implications for mantle composition and processes. In: Saunders AD, Norry MJ (eds) Magmatism in the Ocean Basins. Geological Society Special Publication, pp 313–345

Tegner C, Lesher CE, Larsen LM, Watt WS (1998a) Evidence from the rare-earth-element record of mantle melting for cooling of the Tertiary Iceland Plume. Nature 395:591–594

Tegner C, Duncan RA, Bernstein S, Brooks CK, Bird DK, Storey M (1998b) ^{40}Ar–^{39}Ar geochronology of Tertiary mafic intrusions along the East Greenland rifted margin: relation to flood basalts and the Iceland hotspot track. Earth Planet Sci Lett 156:75–88

Ukstins Peate I, Larsen M, Lesher CE (2003) The transition from sedimentation to flood volcanism in the Kangerlussuaq basin, East Greenland: basaltic pyroclastic volcanism during initial Palaeogene continental break-up. J Geol Soc 160:759–772

White R, McKenzie D (1995) Mantle plumes and flood basalts. J Geophys Res 100:17543–17585

Wolfe C, Bjarnasson I, VanDecar J, Solomon S (1997) Seismic structure of the Iceland mantle plume. Nature 385:245–247

Zhou M-F (1994) PGE distribution in 2.7-Ga layered komatiite flows from the Belingwe greenstone belt, Zimbabwe. Chem Geol 118:155–172